Quantifying the surface properties of enzymatically-made porous starches by using a surface energy analyzer

Juan Manuel Martinez-Alejo[1], Yaiza Benavent-Gil[2], Cristina M. Rosell[2*], Teresa Carvajal[3*], Mario M. Martinez[4,5,6*]

[1]Department of Industrial and Physical Pharmacy, Purdue University, 575 Stadium Mall Drive, West Lafayette, IN 47907, USA

[2]Institute of Agrochemistry and Food Technology (IATA-CSIC), C/Agustin Escardino, 7, Paterna 46980, Valencia, Spain

[3]Department of Agricultural and Biological Engineering, Purdue University, West Lafayette, IN 47907, USA

[4]Whistler Center for Carbohydrate Research, Department of Food Science, Purdue University, 745 Agriculture Mall Drive, West Lafayette, IN 47907, USA.

[5]School of Engineering, University of Guelph, 50 Stone Road East, Guelph, ON N1G 2W1, Canada

[6]Department of Food Science, University of Guelph, 50 Stone Road East, Guelph, ON N1G 2W1, Canada

[*]Corresponding authors: mario.martinez@uoguelph.ca; tcarvaja@purdue.edu; crosell@iata.csic.es

Abstract

The behavior of starch during processing and its performance in products is influenced by the surface energetics/structure of the constituent particles. This work investigates the effect of enzymatically-produced porous maize starch particles on their energetic surface properties using inverse gas chromatography-based surface energy analysis (SEA). Three modified maize starch samples treated with amylase (AM), glucoamylase (AMG) and cyclodextrin-glycosyltransferase (CGT), were used for the study. The dispersive surface energy varied from 36.71 (native) to 43.34 mJ/m^2 (AMG < CGT < AM). Enzyme catalysis resulted in porous starches with a more acidic (AMG) and a more basic (AM) surfaces. CGT exhibited similar acid-base balance as native starch but with higher concentration of active sites on the surface. This is the first study on the surface energy of enzymatically-treated porous starch materials using SEA, revealing significant information regarding the surface interactions that can affect performance of food and pharmaceutical products.

Keywords

surface energetics; porous starch; starch structure; enzymes; inverse gas chromatography; water-sorption;

1 Introduction

Starch is a well-known non-toxic, available, renewable and low-cost source of novel biomaterials and it is one of the first-choice ingredients and excipients in the food and pharmaceutical fields, respectively. Starch is comprised of glucose units joined together by glycosidic bonds. However, the main components of starch, amylose [essentially linear with degree of polymerization (DP) between approximately 600 and 3300] and amylopectin (extensively branched with DP between 4800 and 15,900), are packed into semi-crystalline granules that contain low surface areas and pore volumes (Vamadevan & Bertoft, 2014), which may find limitations in certain applications requiring reagent accessibility or powder flowability. As an example, in the pharmaceutical field, native starch displays poor flow and elastic deformation during tableting, and therefore it is used mostly as a disintegrant.

The development of starches with abundant micro-sized pores, known as porous starches, has been shown to improve significantly the physical retention of liquids throughout the starch granule (Whistler, Madson, Zhao, & Daniel, 1998; Karim, Sufha, & Zaidul, 2008; Benavent-Gil & Rosell, 2017). Porous starch can be obtained by different physical and biological methods (Sujka & Jamroz, 2007), although enzyme treatments are the most widely used. The treatment of maize starch granules with glucoamylase (also known as amyloglucosidase) or α-amylase is for long time known to produce porous starch (Fitt & Snyder 1984) and over the years, other enzymes such as β-amylase, pullulanase, isoamylase and cyclodextrin-glycosyltransferase (CGTase) have also been used (Dura, Błaszczak, & Rosell, 2014; Blazek & Gilbert, 2010; Chen & Zhang, 2010; Benavent-Gil & Rosell, 2017). The size distribution, area of the pores and physical retention of liquids (water and oil absorption capacity) are contingent upon the type of enzyme used for the starch treatment. In particular, Benavent-Gil & Rosell

(2017) reported that glucoamylase leads to porous starches with larger pores (wider diameter), whereas CGTase resulted in pores with significantly smaller diameter. Although it seems that the external pore diameter is positively correlated to the water and oil retention capacity of the porous starch, non-visible interconnecting interior channels have been reported to constitute a cavity capable of carrying 54 % or more weight of substances (Zhao et al. 1996). Interestingly, there are no studies considering both the outer pore diameter and inner porosity, which could be approached by a combination of microscopic observations and the specific surface area (SSA) quantification by means of Inverse Gas Chromatography (IGC).

IGC has proven to be a reliable tool for measuring the surface properties of different solid materials. Although similar in principle to gas chromatography, in IGC, samples are located in the column as stationary phase and different identified non-polar and polar probes are passed through it. The differences in the retention times of the probes with respect to a non-interacting probe (usually methane) can be used to determine different properties, such as SSA, surface energy and acid-base properties (Mohammadi-Jam & Waters 2014; Kondor & Hogan 2017). These parameters have been shown to relate with different processes involving interfacial phenomena, including powder flow, tabletability and wettability (Planinšek, et al., 2003; Chamarthy, Pinal, & Carvajal, 2009; Karde & Ghoroi, 2014).

In the food industry, porous starches are used due to their improved physical retention (absorption) of liquid inside the channels in a sponge-like manner that indirectly protects sensitive elements. In this way, they are used as carriers of colorants, spices, flavorings and sweeteners and also for the protection of oils, minerals, vitamins, bioactive lipids, food pigments such as β-carotene and lycopene which are sensitive to light, oxidation or high temperature (Belingheri, Giussani, Rodriguez-Estrada, Ferrillo,

& Vittadini, 2015; Luo et al., 2013; Majzoobi, Hedayati, & Farahnaky, 2015). On the other hand, porous starches have also been reported to be interesting in the food and pharma industries for their increased reagent accessibility to the hydroxyl groups that bring about potential metal ions-starch coordination or chemical reactions such as esterification or etherification. Therefore, not only the SSA, but also the surface free energy (defined as the excess of energy that is caused by the unbalanced forces between the surface and the bulk) are outstanding parameters that will mark the functionality of porous starches. It could therefore be envisaged that porous starches could show tailored mineral retention (Luo et al., 2013; Baczkowicz et al., 2003; Tomasik & Schilling, 2004; Lii, Tomasik, Hung, & Lai, 2002) or be useful for the development of oral dosage forms with modified drug release. We hypothesized that the surface energy could be significantly altered when using enzymes with different catalytic mechanism, since the granular surface might be comprised by starch molecules with different structure (Martinez & Gomez, 2017a,b).

In the present work, the effect of different enzymes (amylase, CGTase and amyloglucosidase) on macrostructure, SSA, starch fine structure, non-polar (dispersive) and polar surface forces (specific) was studied. In addition, a more detailed study on the acid-base behavior (polar forces) was performed with the aim of obtaining detailed insight on molecular moieties and unbalances forces that would affect the physical features of porous starches. For the first time, different surface properties of enzymatically-made porous starches is reported. Ultimately, this work will provide mechanistic understanding on the use of enzymatically-made porous starches as mineral and drug carriers in food and pharma applications, where physical texture is paramount, encompassing parameters including wettability, powder flowability, agglomeration and tabletability (Grimsey, Feeley, & York, 2002).

2 Materials and Methods

2.1 Materials

In a previous publication by Benavent-Gil and Rosell, 2017, the development and preparation of enzymatically modified porous starches are described in detail. Three of these modified starches were used for the study. In particular, AMG 55 (55 U amyloglucosidase / g starch), AM 55 (55 U amylase /g starch) and CGT 1 (1 U CGTase / g starch) were chosen since they were treated with the highest enzyme activity and expected to show the largest differences in surface properties. In addition, three more samples were used, a native corn starch (Miwon, Seoul, Korea) and two controls that consist of starch samples placed at pH 4.0 (AMG control) and pH 6.0 (AM and CGTase controls) but without being subjected to the action of the enzyme.

All the other chemicals were analytical reagent grade and used without further purification. All solutions and standards were prepared by using deionized water.

2.2 Methods

2.2.1 Particle size distribution

The particle size of each sample after dip-in wet dispersion with the Hydro EV unit was measured with a laser diffraction particle size analyzer Mastersizer 3000 (Malvern Instruments, Worcestershire, UK).

2.2.2 Starch fine molecular structure

The molecular size distributions of debranched starches were analyzed in duplicate using a size exclusion chromatography (SEC) system (Agilent 1260 series, Agilent Technologies, Waldbronn, Germany) equipped with a refractive index detector (RID, 1260 RID, Agilent, Agilent Technologies, Waldbronn, Germany) following the method of Cave, Seabrook, Gidley, and Gilbert (2009) with minor modifications. Starch samples were dissolved in DMSO-0.5% (w/w) LiBr solution (DMSO/LiBr), and

possible remaining non-starch polysaccharide components were then removed by precipitating starch using 6 volumes of ethanol followed by centrifugation at 4000 *g* for 10 min. The precipitated starch was collected and re-dissolved in 0.9 mL of warm deionized water and kept in a boiling water bath for 15 min, cooled down to room temperature, and mixed with 5 µL sodium azide solution (40 mg/mL), 0.1 mL acetate buffer (0.1 M, pH 3.5), and 2.5 µL isoamylase in sequence. The debranching reaction was carried out at 37 °C for 3 h. The debranched starch dispersion was neutralized to pH ~7 with 0.1 M NaOH solution and then heated at 80 °C in a thermomixer for 1 h to inactivate the enzyme. Debranched samples were freeze-dried, dispersed in 1 mL DMSO/LiBr, and injected into PSS GRAM 100 and 1000 columns (PSS GmbH, Mainz, Germany) connected in series, which had a separation range of 100 to ~10^6 Da. An example of a SEC distribution represented as RID signal v elution time is represented in supplementary material 1.

The size distribution was plotted as SEC weight distribution, w[logVh (hydrodynamic volume)], derived from RID signals against Rh. The DP of linear branches was calculated from the Vh using the Mark-Houwink equation (Vilaplana, & Gilbert, 2010). The fine molecular structures of amylopectin branches are reported as the DP at each peak maximum (XAp1 and XAp2), and the peak height of each peak maximum is reported as a ratio to the height of the first amylopectin (Ap) peak maximum (denoted by hAp2/Ap1). The amylose content of maize starch was determined from the SEC molecular size distribution of debranched starch as the ratio of the area under the curve (AUC) of amylose branches to the AUC of overall amylopectin and amylose branches (International Standardization Organization, 2011; Vilaplana, Hasjim, & and Gilbert, 2012).

2.2.3 X-Ray Powder Diffraction (PXRD) patterns

The powder X-Ray diffraction pattern of the samples were analyzed using a Shimadzu 6000 X-ray Diffractometer (Shimadzu) operating at 40 kV and 30 mA, producing CuKa radiation of 0.154 nm wavelength. Diffractograms were obtained by scanning from 3◦ to 40◦ (2theta) at a rate of 2 ◦/min. Relative crystallinity was calculated as the sum of the area of each crystalline peak divided by the total area (both crystalline peaks and amorphous background) using Origin pro 2016 (Origin lab corporation, Northampton, MA, USA.).

2.2.4 Moisture sorption analysis

The moisture sorption isotherms were determined at 25 °C on a symmetrical gravimetric analyzer (Model SGA-100, VTI Corporation, Hialeah, FL, USA) from 10% to 90% RH. The samples were dried on the instrument at 25 °C until constant weight was attained. Sodium chloride and polyvinylpyrrolidone (PVP) were used as calibration standards to ensure the proper functioning of the instrument. Analysis was performed through the range of relative pressure (P/P_0) of 0-0.90 at 25 °C.

2.2.5 Surface energy analysis

All IGC surface energy analysis experiments were carried out using an SMS-IGC 2000 system (Surface Measurement Systems NA, PA, USA) equipped with a flame ionization detector. All IGC analyses were carried out using IGC Surface Energy Analyzer and the data were analyzed using SEA Analysis Software Advanced version 1.4.2.0. For each measurement, pre-silanised glass columns with 30 cm length and 4 mm internal diameter were filled with about 500 mg of the samples and gently packed by tapping. Each column was pre-conditioned *in-situ* for 1 hour at 30 °C and 0% RH with helium carrier gas to remove any physisorbed water. Methane was used as the tracer molecule (dead-time determination). All solvents employed were obtained from Sigma Aldrich (USA) and were of analytical grade.

The SSA of a powder can be determined from applying the linear form of the Brunauer–Emmett–Teller (BET) equation on the isotherm of a gas that weakly interact with a solid, as follow:

$$\frac{p/p^0}{n(1-p/p^0)} = \frac{1}{n_m C} + \frac{C-1}{n_m C}(p/p^0)$$

where p and p^0 are the equilibrium and the saturation pressure of adsorbates at the temperature of adsorption, n is the specific amount adsorbed at the relative pressure p/p^0, n_m is the specific monolayer capacity, and C is the BET constant. The SSA can then be calculated from the equation:

$$SSA = \frac{n_m N_A \sigma_m}{m}$$

Where N_A is Avogadro's number, σ_m is the molecular cross-sectional area of the adsorbing species, and m is the mass of the sample (Thommes et al, 2015).

N_2 isotherms are among the most common gases employed for SSA measurements. However, N_2 measurements in organic materials are problematic due to the difficulty to employ typical degassing conditions and the very low N_2 uptake at the surface of the solid. In this study, the physical adsorption of octane was measured through IGC, since it has proven to be a viable alternative for measuring the SSA, as precondition of the sample (degassing) and experiments can be performed at room temperature and on materials with a SSA below 1 m^2/g (Sharif, DiMemmo, Thommes, Hubert, & Hubert, 2015). SSA of the different samples were determined by measuring the octane adsorption isotherms at 30 °C, 0% RH and with a helium flow rate of 5 standard cm^3/min. The BET surface areas were subsequently calculated from the corresponding octane isotherms within the partial pressure range of 5% to 19% P/P_0.

Surface energy experiments were carried out at different surface coverages. The dispersive energy was determined from the retention time of a series of alkanes (heptane to decane) injected onto the column. Dichloromethane, ethyl acetate, ethanol and

221 acetonitrile were used to determine the specific surface energy (polar). From the
222 retention times of nonpolar and polar probes, a methodology has been established to
223 calculate the powder's surface energy following the next equation:

$$RTlnV_N = 2N_A\alpha\sqrt{\gamma_S^D\gamma_L^D} + C$$

224 Where R is the gas constant (J/mol K), T is the temperature (K), V_N is the net retention
225 volume of the probe (min), N_A is the Avogadro number, α is the cross-sectional area of
226 the probe molecule (m^2), γ_S^D is the dispersive component of the free energy of the solid
227 (J/m2), γ_L^D is the dispersive component of surface free energy of the liquid probe (J/m^2),
228 and C is a constant. The dispersive component of the free energy is thus obtained from
229 the gradient of a plot of RT ln V_N against $\alpha(\gamma_L^D)^{1/2}$. The value of γ_S^D is calculated from
230 $(slope/2N)^2$. The specific contributions for the polar probes are obtained from the
231 specific free energy of adsorption (ΔG) which is the vertical distance of the polar probe
232 from the dispersive probe reference plot (Gamble et al., 2012).

233 **2.2.6 Statistical analysis**

234 Differences among results were studied by analysis of variance (one-way ANOVA).
235 Fisher's least significant difference (LSD) was used to describe means with 95%
236 confidence intervals. The statistical analysis was performed with the Statgraphics
237 Centurion XVI software (Statpoint Technologies, Inc., Warrenton, USA).

238 **3 Results and discussion**

239 **3.1 Granular and supramolecular structure of porous starches**

240 The particle size distribution of the different samples is displayed in Fig. 1. Generally,
241 all samples exhibited a monomodal particle size distribution, with a predominant
242 population of granules with a mean particle diameter of around 14 μm. All starches
243 displayed a rather small population of granules with a mean particle diameter ranging
244 from 0.5 to 3 μm, which could result from some erosion during the process (Jane et al.

1992). Therefore, we can infer that the different treatments to produce porous starches do not cause changes in granule size, which agree with the SEM findings reported by Benavent-Gil & Rosell (2017). Interestingly, only amylase-treated porous starch (AM) exhibited a small population of particles with a mean particle diameter of ~150 μm, suggesting granular aggregation. Dura, Błaszczak, & Rosell (2014) showed some granular aggregation in the SEM micrographs of the starches, but it seems that those granule-granule interactions were weak, because dip-in dispersion with the Mastersizer centrifugal pump before particle size determinations were sufficient to broke them (Fig. 1). In this way, only the resulting action of α-amylase may bring about granular agglomeration, which could be related to surface changes.

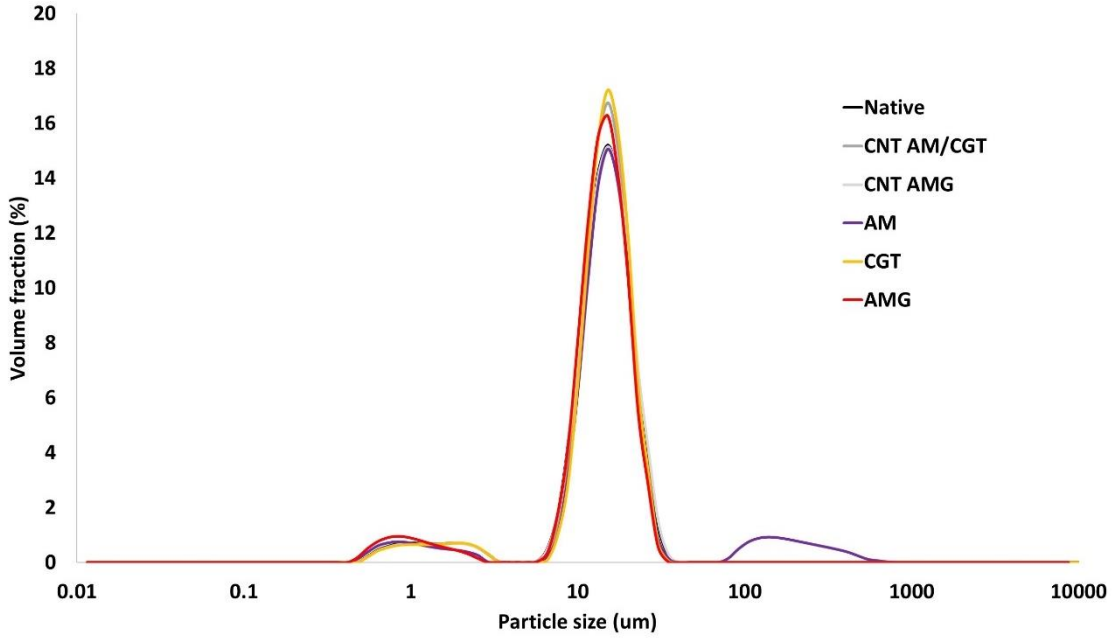

Figure 1. Particle size distributions of native maize starch and porous starches. Abbreviations: CNT: control for AM/CGTase at pH 6.0 or AMG at pH 4.0; porous starches were obtained by treatment with amylase (AM), amyloglucosidase (AMG) or cyclodextrin glycoxyl transferase (CGT).

Starch samples were analyzed to report potential variations in the proportion of crystalline and amorphous regions that could impart differences in the starch adsorptive capacity and/or surface properties. All samples exhibited a typical A-type pattern (Fig. 2), whose main peaks are allocated at 2θ of around 14.9^{o}, 17.0^{o}, 17.9^{o}, and 23.0^{o} (Lopez-Rubio, et al., 2008). The relative crystallinity calculated (area of the crystalline peaks divided by the total area of the diffractogram) showed no significant differences among them, except for CGTase-treated porous starch (Table 1). A side-by-side and even hydrolysis mechanism of amylase starting from the channels was suggested by Zhang et al. (2006) in maize starch, which was suggested to likely result in a simultaneous hydrolysis of crystalline and amorphous regions. However, it seems that CGTase impaired an even hydrolysis of crystalline and amorphous fractions, the latter being significantly more hydrolyzed (as seen by the higher relative crystallinity). In fact, Benavent-Gil and Rosell (2017) explained the pore morphology indicating that CGTase, and in less extent AM, attacked a higher proportion of amylose, leading an increase in the amount of amylopectin, suggesting deeper pinholes and the attack of amorphous and

277 crystalline structure.

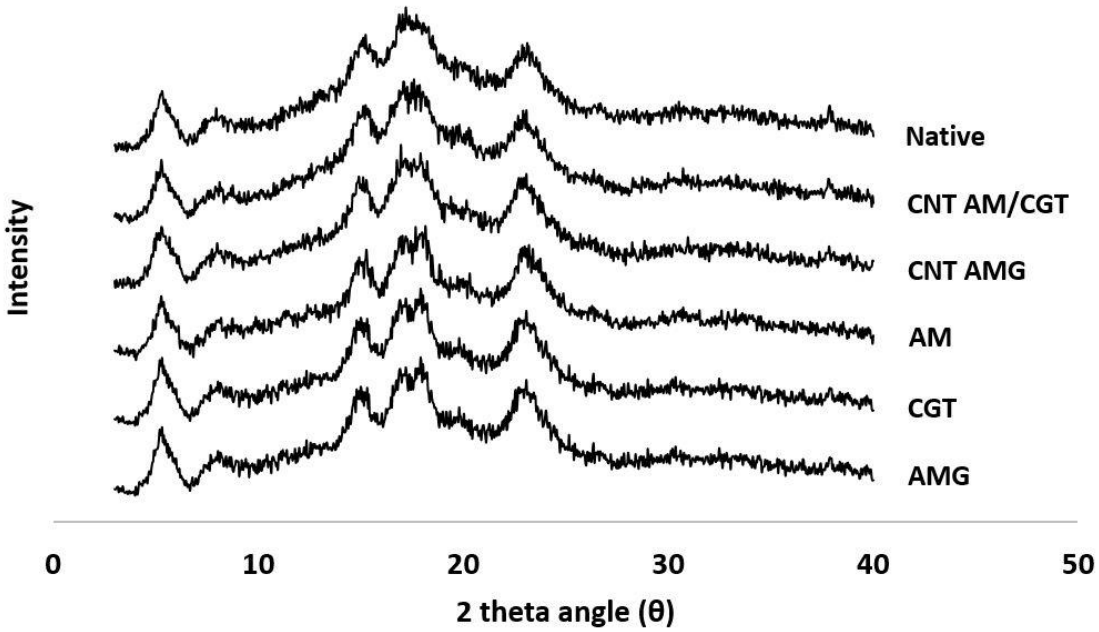

278

279 **Figure 2.** PXRD diffraction pattern.

280 In order to measure the changes in the area endowed by the enzymatic catalysis, we
281 determined the SSA of the samples by means of the BET equation. The SSA values of
282 the native and control samples showed no significant differences among them, whereas
283 the samples treated with enzymes showed higher SSA (see table 1). The tendency in
284 SSA values observed (AM > AMG > CGT > Native/Controls) can be related with the
285 pore sizes induced by the different enzymes (Benavent-Gil & Rosell, 2017).
286 Nevertheless, the relatively high SSA of CGTase-treated porous starch contrasts with
287 the small superficial pore area (reported in Fig. 1r by Benavent-Gil & Rosell, 2017),
288 which reinforces the hypothesis that CGTase-treated granules were extensively
289 hydrolyzed in an inside-out manner.

290

291 **Table 1.** Relative crystallinity (RC) and specific surface area (SSA) of native and
292 enzymatically-treated porous starches.

Starch	RC (%)	SSA (m^2/g)
Native	21.7 ± 0.2 ab	1.74 ± 0.04 a
CNT AM/CGT	20.1 ± 2.8 a	1.83 ± 0.10 a
CNT AMG	23.7 ± 0.5 b	1.64± 0.19 a
AM	22.1 ± 0.0 ab	2.53 ± 0.24 c
CGT	27.2 ± 0.4 c	1.96± 0.15 ab
AMG	19.3 ± 0.7 a	2.25 ± 0.18 bc

Values with different letters in the same column are significantly different with P <0.05. CNT AM/CGT, sample treated at pH 6 (pH for amylase and cyclodextrin-glycosyltransferase treatments) without enzyme; CNT AMG, sample treated at pH 4 (pH for amyloglucosidase treatment) without enzyme; AM, amylase-treated porous starch; CGT, cyclodextrin-glycosyltransferase-treated porous starch; AMG, amyloglucosidase-treated porous starch.

3.2 Unit chain length distribution of starch molecules

Molecular size distributions were normalized to yield the same height of the highest peak to expose detailed features and to facilitate qualitative comparison and interpretation (Fig. 3). The chain length distributions of starch molecules showed three peaks representing short (peak Rh ~1.5 nm or DP ~16) and long (peak Rh ~2.5 nm, DP ~50) amylopectin chains as well as amylose chains (Rh ~5–80 nm, DP ~100–10,000) (Wang, Hasjim, Wu, Henry, & Gilbert, 2014). Short amylopectin branches are supposed to be a mixture of short B-chains (B1-chains) and A-chains whereas long amylopectin branches represent B-chains (B2, B3, etc) (Perez & Bertoft, 2010). Albeit no differences were found in the average length of short and long amylopectin chains, a significantly lower long to short amylopectin chains molar ratio was found in CGT sample (0.48) compared to the others (~0.56), which can be seen in Fig. 3. Interestingly, this suggests that the amorphous fraction of CGTase-treated starch granules was removed by simultaneous hydrolysis of amylose and long chains from the amylopectin backbone (B2+B3, etc). In fact, since hydrated amylopectin molecules within starch granules may

behave as a liquid-crystalline polymer, this would entail a removal of spatial constraints and allow double helices to align into more crystalline structures (Vermeylen et al., 2004; Wang et al., 2012), which may also explain the increase in the relative crystallinity of CGT sample (Table 1).

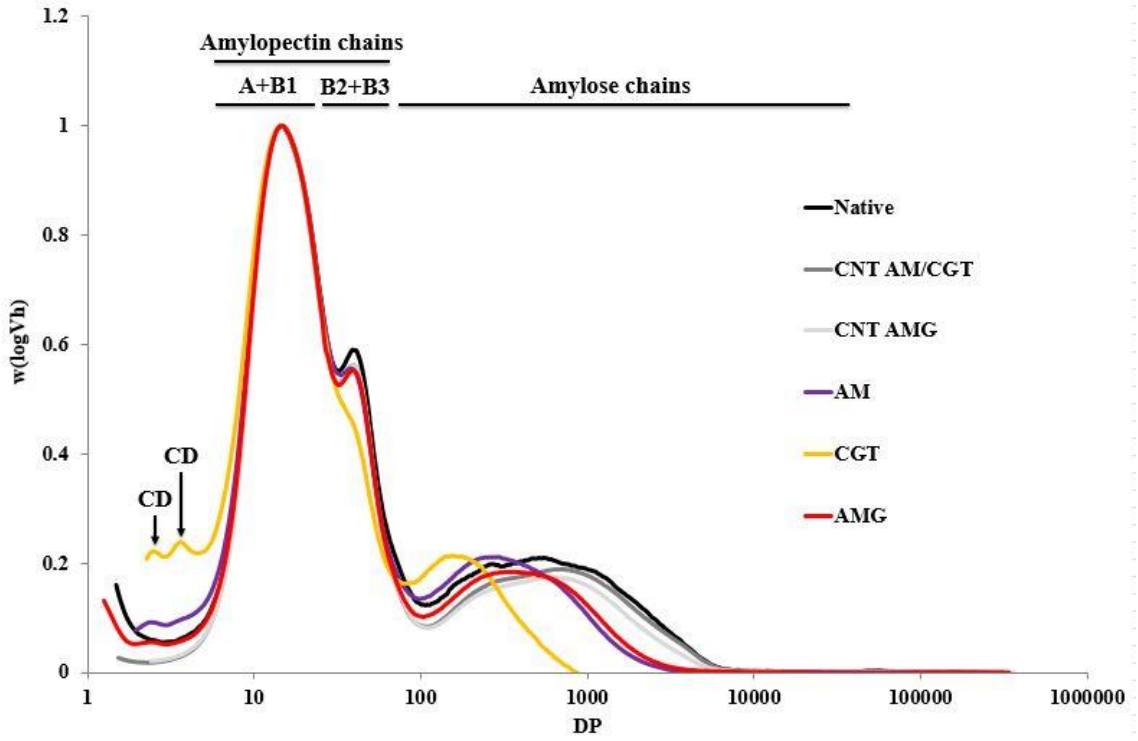

Figure 3. Molecular size distribution of debranched native maize and porous starches. CNT AM/CGT, sample treated at pH 6 (pH for amylase and cyclodextrin-glycosyltransferase treatments) without enzyme; CNT AMG, sample treated at pH 4 (pH for amyloglucosidase treatment) without enzyme; AM, amylase-treated porous starch; CGT, cyclodextrin-glycosyltransferase-treated porous starch; AMG, amyloglucosidase-treated porous starch. CD, cyclodextrins.

The average amylose length (DP at peak maximum) represented in Fig. 3 was lower for CGTase-treated starch [DP = 152 glucose units (GU)], followed by amylose from AM (292 GU) and AMG samples (364 GU). Results also showed a significantly lower amylose size of enzyme-treated samples with respect to native and control samples

(550-700 GU). Since all samples come from the same material (maize starch), a shorter amylose length would reflect a more extensive amylose hydrolysis.

It is important to mention that molecular size of starch branches was analyzed to the whole population of starch molecules, i.e. molecules located both in the inner part of the granule and on its surface. Therefore, variations in the molecular structure as a result of amylolysis are partially masked by the intact starch molecules present in the crystalline and less accessible parts of the granule.

3.3 Water sorption isotherms

The water sorption-desorption isotherms for the various modified (porous) corn starches are shown in Fig. 4. The isotherms for the modified, as well as the control and native starches, were very similar. The similarity of the sorption isotherms indicates that the change in surface area induced by the presence of pores in the modified starches has a minimal effect on water vapor sorption. On the other hand, when the same modified materials were exposed to bulk (liquid) water, their water-saturation uptake capacity was different (Benavent-Gil & Rosell, 2017). The water sorption profiles show no evidence of water vapor condensation in the pores of the modified starches, based on the similarity of the isotherms between the samples. Additional studies are needed in order to explain the difference in water uptake observed in the water-saturated samples but not observed from vapor sorption. However, a reasonable explanation, based on capillary phenomena, could be related to the geometry (radius and volume) of the pores that makes them effective reservoirs for bulk (liquid) water but no adequate to promote water condensation from the vapor.

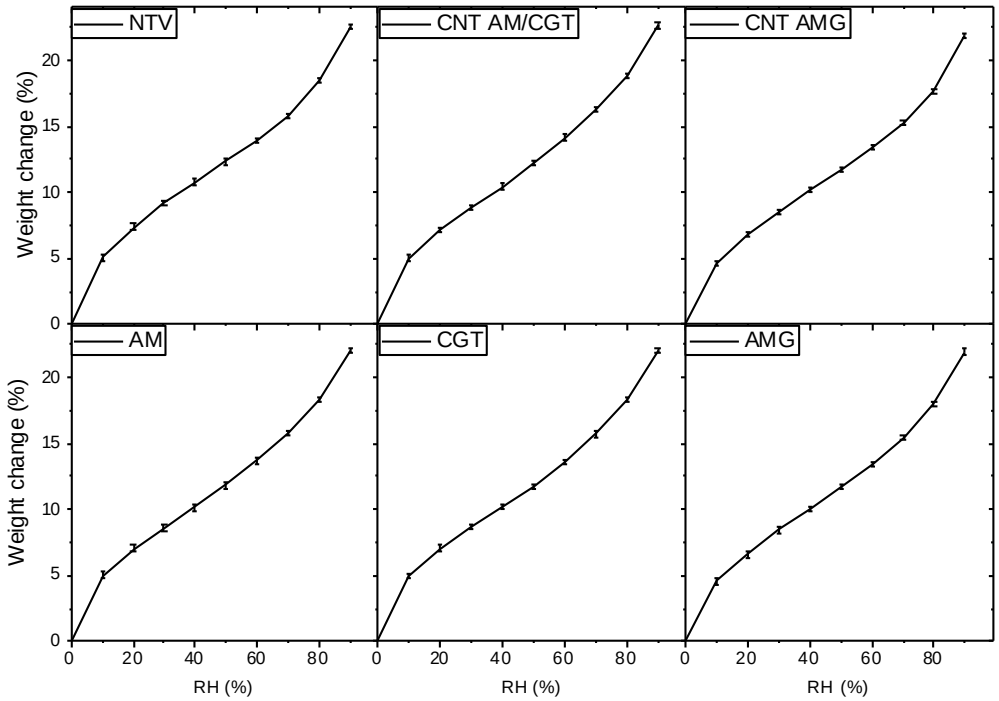

355

356

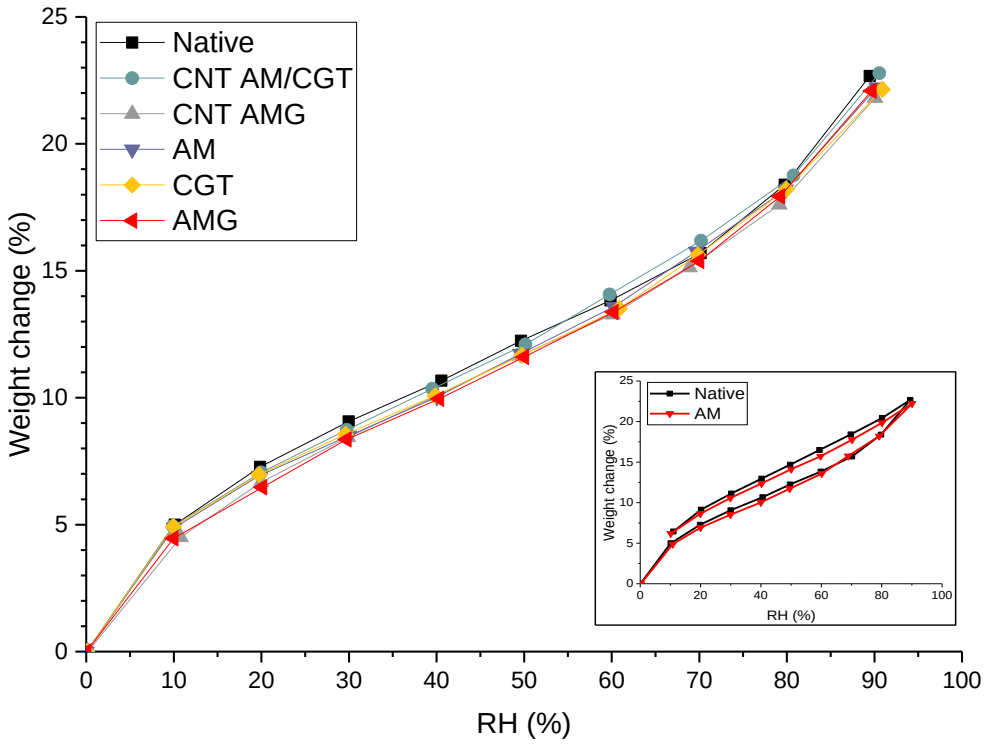

357

358 **Figure 4.** Water-sorption isotherms at 25 °C of the different powder porous starches. (a)

359 individual isotherms; (b) direct comparison of the isotherms.

360

3.4 Surface energy

Surface energy, which is the excess of energy associated with a surface, was evaluated to characterize the solid surface. The surface energy is caused by the unbalanced forces between the surface and the bulk. The total surface free energy is the result of the non-polar forces (dispersive) and polar forces (specific), and therefore, it is sensitive to the surface chemical composition (Ho & Heng, 2013). Surface energy determinations have been traditionally assessed by contact angle measurements, but this method is designed for flat homogeneous materials (Parsons, Buckton, & Chatman, 1992). In this study, the surface energy was tested by means of IGC, which has been proven to be suitable for analyzing powders regardless of their chemical nature, surface heterogeneity, surface area and porosity (Sunkersett et al., 2001; Lapčík et al., 2016).

Fig. 5 shows the combined plot of the dispersive, polar and total surface energy as a function of the surface coverage of the different starches analyzed (surface energy heterogeneity map). The surface energy of the starches is governed mostly by dispersive forces (values >30 mJ/m^2), with a polar contribution of approximately 5 mJ/m^2. Native, AM, AMG and CGT samples displayed a heterogeneous profile characterized by high surface energy values that diminish as the surface coverage increases. On the other hand, CNT AM/CGT and CNT AMG showed a homogeneous surface energy distribution through all the surface coverage measured, indicating a smoothening of the surface due to the incubation process. This phenomenon could be related to the presence of water, since it has shown to induce changes in both polar and dispersive components (Sunkersett et al., 2001; Papirer, Brendle, Balard, & Vergelati, 2000).

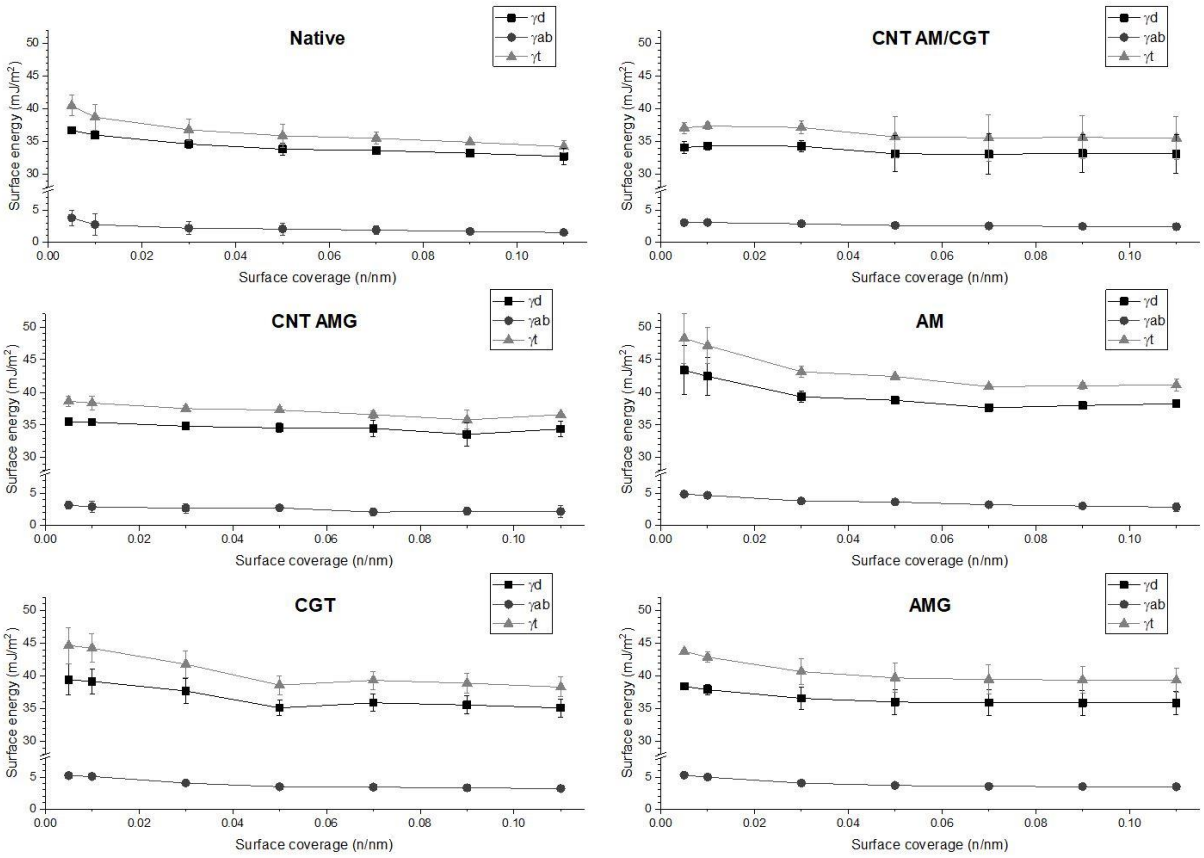

Figure 5. Surface energy heterogeneity of the different starches studied herein. γd, dispersive energy; γab, specific surface energy; γt, total surface energy (scale in y axis is split for clarity).

With the intention to provide further understanding of the differences between the starches, we performed a more detailed analysis at 0.05 of surface coverage (Table 2). This zone was selected due to the higher energetic sites observed in the samples. The dispersive surface energy corresponds to the non-specific interactions, whereas the specific surface energy relates to the contribution of polar intermolecular forces. The total surface energy is the sum of the dispersive and specific surface energy. Values of K_a, K_b and the K_a/K_b ratio indicate the ability of a surface to interact by specific Lewis acid-base forces. No significant differences in the surface energy (dispersive, specific and total) were found among native and control samples (CNT AM/CGT and CNT AMG). However, significant higher values were obtained for the enzymatically-treated

samples. Among these, the highest dispersive energy was observed for AM, followed by CGT and AMG. On the other hand, no significant differences were observed in the specific surface energy for those enzymatically treated samples. The total surface energy is the combination of the dispersive and specific values obtained, and therefore, its values depend of the magnitude of both. Thus, the trend AM>CGT>AMG observed for the total surface energy indicate that, for these samples, this parameter is the reflection mostly of the dispersive component. The increase of the dispersive energy in AM could be the reason behind the granular aggregation observed during the particle size determinations, as polar components at the surface has shown to promote a better wettability in comparison to a surface dominated by hydrophobic components (Kondor & Hogan, 2017).

Table 2. Surface energy of the different starch samples analyzed at infinite dilution.

	NATIVE	CNT AM/CGT	CNT AMG	AM	CGT	AMG
Dispersive Surface Energy (mJ/m^2)	36.71 ± 0.40abc	34.1 ± 0.89a	35.48 ± 0.28ab	43.34 ± 3.71d	39.43 ± 2.35cd	38.42 ± 0.21bc
Specific surface energy (mJ/m^2)	3.78 ± 1.19ab	3.02 ± 0.04a	3.15 ± 0.60a	4.88 ± 0.08bc	5.23 ± 0.40c	5.31 ± 0.01c
Total surface energy (mJ/m^2)	40.49 ± 1.58ab	37.12 ± 0.85a	38.63 ± 0.79a	48.25 ± 3.83c	44.66 ± 2.75bc	43.73 ± 0.23bc
Acid constant (K_a)	0.07 ± 0.02a	0.09 ± 0.01ab	0.08 ± 0.02a	0.13 ± 0.00c	0.12 ± 0.00bc	0.08 ± 0.00a
Base constant (K_b)	0.18 ± 0.09a	0.18 ± 0.03a	0.17 ± 0.04a	0.18 ± 0.02a	0.23 ± 0.00ab	0.30 ± 0.05b
Ratio (K_a/K_b)	0.43 ± 0.09ab	0.51 ± 0.04b	0.51 ± 0.14b	0.76 ± 0.13c	0.51 ± 0.01b	0.27 ± 0.04a

Values with different letters in the same row are significantly different with $P < 0.05$. CNT AM/CGT, sample treated at pH 6 (pH for amylase and cyclodextrin-glycosyltransferase treatments) without enzyme; CNT AMG, sample treated at pH 4 (pH for amyloglucosidase treatment) without enzyme; AM, amylase-treated porous starch; CGT, cyclodextrin-glycosyltransferase-treated porous starch; AMG, amyloglucosidase-treated porous starch.

The changes observed in the dispersive and total surface energy would seem to indicate that the surface energy is directly related with the SSA, however, they are independent.

SSA changes indicate the presence of larger number of units per area, whereas an increase in the surface energy is the result of a larger expression of active sites or the same amount of sites but more reactive per surface area (Yao, et al., 2015). The amorphous/crystalline content of the sample, and the chemical composition (functional groups) at the surface are plausible explanations behind the increase in the surface energy values obtained (Cordeiro, Gouveia, Morales, & Amico, 2011). However, the lack of differences in the PXRD pattern between the samples studied herein show that the changes observed in the surface energy do not derive from changes in their amorphous content, but rather from the chemical modifications entitled by the enzymes on the samples. Therefore, these results indicate that the enzymatic treatment induce simultaneously the generation of pores, reflected in an increase in the SSA, and the formation of new higher energetic interaction sites (dispersive and polar).

From the surface free energy of the polar probes, and by using the Gutmann approach, the acid (K_a) and base number (K_b) of the starches were calculated (Mohammadi-Jam & Waters, 2014). This type of analysis provides information related to the orientation of functional groups at the surface of the powder and the acidic/basic character of the surface of a solid. K_a is related to the acidic or electron accepting capacity of the surface, whereas K_b describe the basic or electron donating capacity. The K_a/K_b ratio can be used to classify a surface as acid ($K_a/K_b > 1$), basic ($K_a/K_b < 1$), or amphoteric ($K_a/K_b \approx 1$) (Buckton & Gill, 2007). Additional differences between samples can be observed from the interaction energy of the polar solvents injected. In most cases, significant changes were detected in the measurements not only with regards to the native/control samples, but also, between the modified starches. This set of energetic values allows to discriminate between samples, which demonstrate that the IGC is a sensitive tool to detect the surface alterations endowed by the enzymes. All the starches

showed a K_a/K_b ratio <1, which indicate that the electron donating groups prevails over electron acceptor groups at the surface of the solid (i.e. basic). Native and control samples showed minor differences in their values for K_a, K_b and K_a/K_b, which demonstrates that the reaction conditions (without enzyme) does promote minimal changes in the overall surface energy of the starch, and that the changes observed in the surface of porous starches are solely derived from the action of the different hydrolases employed. When using enzymes, AMG sample almost doubled its K_b while maintaining K_a constant. CGT on the other hand, did not promote significant effect on both K_a and K_b of its respective control, whereas AM, did only increase its K_a value, leading to a significant increase of K_a/K_b. Results seem to indicate that an increase in the electron donating capacity (Lewis base behavior) is attained with the use of exo-acting hydrolases (amyloglucosidase), which also resulted in lower dispersive surface energy, compared to the other enzymatically treated starches. Considering the overall surface acid-base behavior (K_a/K_b), the enzyme catalysis resulted in porous starches with a more acidic and a more basic surface in AMG and AM samples, respectively, and one surface analogous to that of native starch but with more acid and basic active sites on the surface (CGT).

This alteration of the surface chemistry, surface energy and surface acid-base behavior has shown to be valuable in different fields (Grimsey et al., 2002). For instance, due to its biodegradable nature, starch is a desired additive in the mineral industry to flocculate and depress the flotation of certain minerals, but it has the disadvantage that its behavior can be unpredictable and non-selective towards them. In this regard, it has been studied that the interaction between the polysaccharides and ions is driven by acid-base interactions between the surface functional groups at the surface of the starch (hydroxyl

and aldehyde groups) and the nature (size and valence) of the mineral (Liu, Zhang, & Laskowski, 2000).

Conclusions

The suitability of porous starch granules as mineral and drug carriers may rely on different physicochemical features including their surface properties, such as the specific surface area, surface free energy and acidic/basic behavior. The analysis performed by IGC showed that the measurements from the probes injected are sensitive enough to detect the changes in the specific surface area and energy of the porous starches. The IGC measurement allowed also to infer that the changes in the surface energy are the results of new higher energetic sites available at the surface of the starch. This study also highlights how the mechanistic process carried out by the enzymes tune the final outcomes obtained at the surface of the starch. IGC results also exhibited that the enzyme catalysis resulted in porous starches with a more acidic and a more basic surface in AMG and AM samples, respectively, and one surface analogous to that of native starch (CGT).

Acknowledgements

JMMA acknowledges the financial support from COMEXUS (Fulbright-Garcia Robles scholarship), Consejo Nacional de Ciencia y Tecnología (CONACYT), to Prof. Rodolfo Pinal of Industrial and Physical Pharmacy at Purdue University and the Center for Pharmaceutical Processing Research (CPPR) for the postdoctoral research scholarship. CMR and YB-G acknowledge the financial support of the Spanish Ministry of Economy and Competitiveness (Project AGL2014-52928-C2-1-R) and the European

Regional Development Fund (FEDER). YB-G would like to thank predoctoral fellowship from Spanish Ministry of Economy and Competitiveness.

References

Baczkowicz, M., Wójtowicz, D., Anderegg, J. W., Schilling, C. H., & Tomasik, P. Starch complexes with bismuth(III) and (V). *Carbohydrate Polymers*. 2003, 52, 263−268.

Belingheri, C., Giussani, B., Rodriguez-Estrada, M. T., Ferrillo, A., & Vittadini, E. (2015). Oxidative stability of high-oleic sunflower oil in a porous starch carrier. *Food Chemistry*, 166, 346–351.

Benavent-Gil, Y., & Rosell, C. M. (2017). Comparison of porous starches obtained from different enzyme types and levels. *Carbohydrate Polymers*, 157, 533-540.

Blazek, J., & Gilbert, E. P. (2010) Effect of enzymatic hydrolysis on native starch granule structure, *Biomacromolecules.* 11(12), 3275–3289.

Buckton, G., & Gill, H. (2007). The importance of surface energetics of powders for drug delivery and the establishment of inverse gas chromatography. *Advanced Drug Delivery Reviews*, 59(14), 1474–1479.

Cave, R. A., Seabrook, S. A., Gidley, M. J., & Gilbert, R. G. (2009). Characterization of starch by size-exclusion chromatography: the limitations imposed by shear scission. *Biomacromolecules*, 10(8), 2245-2253.

Chamarthy, S. P., Pinal, R., & Carvajal, M. T. (2009). Elucidating raw material variability--importance of surface properties and functionality in pharmaceutical powders. *AAPS PharmSciTech*, 10(3), 780–788.

Chen, G., & Zhang, B. (2012). Hydrolysis of granular corn starch with controlled pore size, *Journal of Cereal Science*, 56 (2), 316–320.

Cordeiro, N., Gouveia, C., Moraes, A. G. O., & Amico, S. C. (2011). Natural fibers characterization by inverse gas chromatography. *Carbohydrate Polymers*, *84*(1), 110–117.

Dura, A., Błaszczak, W., & Rosell, C. M. (2014). Functionality of porous starch obtained by amylase or amyloglucosidase treatments. *Carbohydrate Polymers*, 101, 837–845.

Fitt, L. E., & Snyder, E. M. (1984). Photomicrographs of starch. In R. L. Whistler, J. N. BeMiller and E. F. Paschall (Eds.), *Starch Chemistry and Technology* (pp. 675-689). Academic Press: New York.

Gamble, J. F., Leane, M., Olusanmi, D., Tobyn, M., Šupuk, E., Khoo, J., & Naderi, M. (2012). Surface energy analysis as a tool to probe the surface energy characteristics of micronized materials - A comparison with inverse gas chromatography. *International Journals of Pharmaceutics*, 422(1), 238–244.

Grimsey, I., Feeley, J., & York, P. (2002). Analysis of the surface energy of pharmaceutical powders by inverse gas chromatography. Journal of Pharmaceutical Sciences, 91(2), 571–583.

Ho, R., & Heng, J. (2013). A Review of Inverse Gas Chromatography and its Development as a Tool to Characterize Anisotropic Surface Properties of Pharmaceutical Solids. *KONA Powder and Particle Journal*, 30, 164–180.

Jane, J. L., Shen, L., Wang, L., & Maningat, C. C. (1992). Preparation and properties of small-particle corn starch. Cereal Chemistry, 69(3), 280-283.

Karde, V., & Ghoroi, C. (2014). Influence of surface modification on wettability and surface energy characteristics of pharmaceutical excipient powders. *International Journal of Pharmaceutics*, 475(1-2), 351–363.

Karim, A. A., Sufha, E. H., & Zaidul, I. S. M. (2008). Dual modification of starch via partial enzymatic hydrolysis in the granular state and subsequent hydroxypropylation. *Journal of Agricultural and Food Chemistry*, 56, 10901−10907.

Kondor A., & Hogan S.A. (2017). Relationships between surface energy analysis and functional characteristics of dairy powders. *Food Chemistry*, 237, 1155–1162.

Lapčík, L., Otyepka, M., Otyepková, E., Lapčíková, B., Gabriel, R., Gavenda, A., & Prudilová, B. (2016). Surface heterogeneity: Information from inverse gas chromatography and application to model pharmaceutical substances. *Current Opinion in Colloid & Interface Science*, 24, 64–71.

Lii, C., Tomasik, P., Hung, W. L., & Lai, V. M. F. (2002). Revised look at the interaction of starch with electrolyte: effect of salts of metals from the first non-transition group. *Food Hydrocolloids*, 16, 35−45.

Liu, Q., Zhang, Y., & Laskowski, J. S. (2000). The adsorption of polysaccharides onto mineral surfaces: an acid/base interaction. *International Journal of Mineral Processing*. 60, 229-245.

Lopez-Rubio, A., Flanagan, B. M., Gilbert, E. P., & Gidley, M. J. (2008). A novel approach for calculating starch crystallinity and its correlation with double helix content: a combined XRD and NMR study. *Biopolymers*, 89, 761-768.

Luo, Z., Cheng, W., Chen, H., Fu, X., Peng, X., Luo, F., et al. (2013). Preparation and properties of enzyme-modified cassava starch-zinc complexes. *Journal of Agricultural and Food Chemistry*, 61(19), 4631–4638.

564 Martinez, M. M., & Gómez, M. (2017a). Insight of the α-Amylase Family of Enzymes:
565 Endo- and Exo-Acting α,1-4 Hydrolases. *Microbial Enzyme Technology & Food*
566 *Applications*. Edited by Ramesh C. Ray and Cristina M. Rosell. CRC Press/ Taylor &
567 Francis Group.
568 Martínez, M. M., & Gómez, M. (2017b). Starch-active Debranching and α-
569 Glucanotransferase Enzymes. In: *Microbial Enzyme Technology in Food Applications*,
570 Edited by Ramesh C. Ray and Cristina M. Rosell. CRC Press/ Taylor & Francis Group.
571 Majzoobi, M., Hedayati, S., & Farahnaky, A. (2015). Functional properties
572 ofmicroporous wheat starch produced by α-amylase and sonication. FoodBioscience,
573 11, 79–84.
574 Mohammadi-Jam, S., & Waters, K.E. (2014) Inverse gas chromatography applications:
575 A review. *Advances in Colloid and Interface Science*. 212,21-44.
576 Papirer, Brendle, Balard, & Vergelati. (2000). Inverse gas chromatography investigation
577 of the surface properties of cellulose. *Journal of Adhesion Science and*
578 *Technology*, 14(3), 321–337.
579 Parsons, G., Buckton, G., & Chatham, S. (1992). The extent of the errors associated
580 with contact angles obtained using liquid penetration experiments. *International*
581 *Journal of Pharmaceutics*, 82(1-2), 145–150.
582 Perez, S., & Bertoft, E. (2010). The molecular structures of starch components and their
583 contribution to the architecture of starch granules: A comprehensive review. *Starch* 62,
584 389-420.
585 Planinšek, O., Zadnik, J., Rozman, Š., Kunaver, M., Dreu, R., & Srčič, S. (2003).
586 Influence of inverse gas chromatography measurement conditions on surface energy
587 parameters of lactose monohydrate. *International Journal of Pharmaceutics*, 256(1-2),
588 17–23.

589 Sharif, S., DiMemmo, L., Thommes, M., Hubert, M., & Sarsfield, B. (2015). A
590 simplified approach to determine effective surface area and porosity of low bulk density
591 active pharmaceutical ingredients in early development. *Advanced Powder Technology*,
592 26(2), 337–348.
593 Sujka, M., & Jamroz, J. (2007). Starch granule porosity and its changes by means of
594 amylolysis. *International Agrophysics* 21, 107-113.
595 Sunkersett, M. R., Grimsey, I. M., Doughty, S. W., Osborn, J. C., York, P., & Rowe, R.
596 C. (2001). The changes in surface energetics with relative humidity of carbamazepine
597 and paracetamol as measured by inverse gas chromatography. *European Journal of*
598 *Pharmaceutical Sciences*, 13(2), 219–25.
599 Thommes, M., Kaneko, K., Neimark, A., Olivier, J., Rodriguez-Reinoso, F., Rouquerol,
600 J., & Sing, K. (2015). Physisorption of gases, with special reference to the evaluation of
601 surface area and pore size distribution (IUPAC Technical Report). *Pure and Applied*
602 *Chemistry*, 87(9-10), 1051–1069.
603 Tomasik, P., & Schilling, C. H. (2004). Chemical modification of starch. In Horton, D.
604 (Ed), *Advances in Carbohydrate Chemistry and Biochemistry*., 59, 175−403.
605 Vamadevan, V., & Bertoft, E. (2014). Structure-function relationships of starch
606 components. *Starch*, 66, 1-14.
607 Vermeylen, R., Goderis, B., Reynaers, H. & Delcour, J. A. (2004). Amylopectin
608 molecular structure reflected in macromolecular organization of granular starch.
609 *Biomacromolecules*, 5, 1775-1786.
610 Vilaplana, F., & Gilbert, R. G. (2010). Characterization of branched polysaccharides
611 using multiple-detection size separation techniques. *Journal of Separation Science*, 33,
612 3537–3554.

Vilaplana, F., Hasjim, J., & Gilbert, R. G. (2012). Amylose content in starches: Towards optimal definition and validating experimental methods. *Carbohydrate Polymers*, 88, 103–111.

Wang, S. J., Blazek, J., Gilbert, E. P. & Copeland, L. (2012). New insights on the mechanism acid degradation of pea starch. *Carbohydrate Polymers*, 87, 1941–1949.

Wang, K., Hasjim, J., Wu, A. C., Henry, R. J., & Gilbert, R. G. (2014). Variation in amylose fine structure of starches from different botanical sources. *Journal of Agricultural and Food Chemistry*, 62, 4443-4453.

Whistler, R. L., Madson, M. A., Zhao, J., & Daniel, J. R. (1998). Surface derivatization of corn starch granules. *Cereal Chemistry*. 75, 72−74.

Yao, Z., Ge, L., Yang, W., Xia, M., Ji, X., Jin, M., Tang, M., & Dienstmaier, J. (2015). Finite dilution inverse gas chromatography as a versatile tool to determine the surface properties of biofillers for plastic composite applications. *Analytical Chemistry*, 87(13), 6724–6729.

Zhang, G., Ao, Z., & Hamaker, B. R. (2006). Slow digestion property of native cereal starches. *Biomacromolecules*, 7(11), 3252-3258.

Zhao, J., Madson, M. A., & Whistler R. L. (1996). Cavities in porous corn starch provide a large storage capacity. *Cereal Chemistry*, 73, 379-380.

Figure captions

Figure 1. Particle size distributions of native maize starch and porous starches.

Figure 2. PXRD diffraction pattern.

Figure 3. Molecular size distribution of debranched native maize and porous starches.

Figure 4. Water sorption isotherms at 25 ^{o}C of the different powder porous starches.

Figure 5. Surface energy heterogeneity of the different starches studied herein. γd, dispersive energy; γab, specific surface energy; γt, total surface energy (scale in y axis is split for clarity).